EAN 2020
58th conference on experimental stress analysis

Residual Stresses of Laser-Hardened Railway Axles

TROJAN K.[1,a], ČAPEK J.[1,b], GANEV N.[1,c], ČERNÝ I.[2,d], KEC J.[2,e], NĚMEČEK S.[3,f]

[1]Department of Solid State Engineering, Faculty of Nuclear Sciences and Physical Engineering, Czech Technical University in Prague, Trojanova 13, 120 00 Prague, Czech Republic

[2]SVÚM a.s., Tovární 2053, 250 88 Čelákovice, Czech Republic

[3]RAPTECH s.r.o., U Vodárny 473, 330 08 Zruč-Senec, Czech Republic

[a]karel.trojan@fjfi.cvut.cz, [b]jiri.capek@fjfi.cvut.cz, [c]nikolaj.ganev@fjfi.cvut.cz, [d]ivo.cerny@seznam.cz, [e]kec@svum.cz, [f]nemecek@raptech.cz

Keywords: Railway axles, Laser hardening, Residual stresses, Fatigue testing

Abstract. The paper describes the influence of laser hardening on the state of residual stresses and high-cycle fatigue resistance of railway axles made of the EA1N steel. It has been found that the compressive residual stresses along the surface of the hardened track in axial direction, which is more important from the technological point of view, significantly increase fatigue strength. With the optimized position of the laser tracks on the inner edge of the axle seats, these compressive stresses can play a crucial role in significantly increasing the fatigue resistance of the axles under operation.

Introduction

This research is aimed at the development of the technology of surface treatment of axles using laser hardening to increase resistance to fatigue failure under press fits. Railway non-powered axles made of standard EA1N steel were examined. These axles are connected with wheels by press fitting, performed usually at room temperature. Failures with fatal consequences can occur on the axle seats due to ongoing mechanical processes during operation [1]. The stress on the axle seats has the character of both high-cycle to very high-cycle fatigue and fretting fatigue. Both mechanisms, in particular, the fretting fatigue mechanism under compression, develop over a large number of load cycles – considering the service life of railway vehicles even more than 10^8 cycles [2]. By researching optimum combinations of laser surface treatment parameters, it is anticipated to achieve optimum structure and surface properties of the axle at critical points, including particularly fatigue resistance being positively affected by compressive residual stresses. Therefore, it is necessary to demonstrate a sufficient state of residual stresses on the axle seats and the higher fatigue life of the axle.

Experiment

For experimental tests, a forged turned semi-finished product made of the EA1N steel was used, see Fig. 1. The hardening was carried out circumferentially, following the expected hardening method for the axles to be operated, on axle seats with a controlled hardening temperature of 1150 °C, and a beam speed of 3 mm/s. Part of the sample was air-quenched, as is common for laser hardening, the second set of experimental samples were cooled with a water spray.

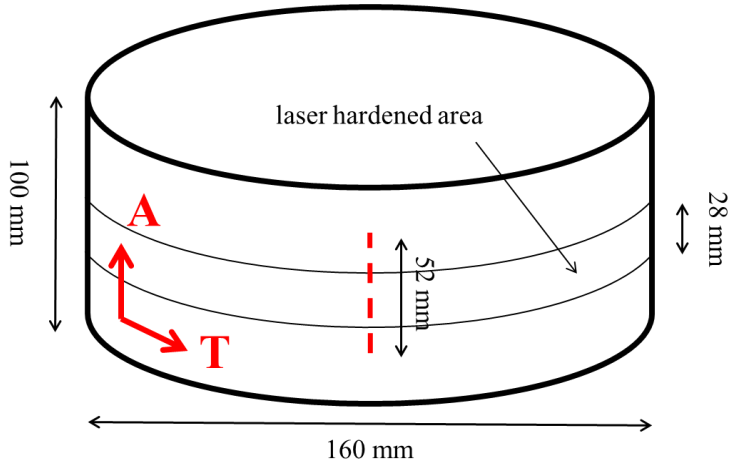

Fig. 1: Diagram of analysed samples

Metallographic specimens were hot embedded into conductive bakelite resin with the carbon filler. After the embedding, the specimens were prepared by machine grinding and polishing. Structure was revealed by etching in 4 % Nital (98 ml ethanol + 2 ml HNO_3). Microstructure was investigated by optical microscope Zeiss Axio Observer Z1M.

Residual stresses were determined by X-ray diffraction, {*211*} diffraction line of α-Fe was measured using Cr*Kα* radiation. The residual stresses across the hardened track, see Fig. 2 and the dashed line in Fig. 1, and consequently, the depth profiles of residual stresses were determined in the middle of the hardened track. The values of residual stresses were calculated from lattice deformations determined on the basis of experimental dependencies of $2\theta(\sin^2\psi)$ assuming uniaxial and resp. biaxial state of residual stress (θ is the diffraction angle, ψ the angle between the sample surface and the diffracting lattice planes). The diffraction angle was determined as the centre of gravity of the Cr$K\alpha_1\alpha_2$ doublet diffracted by the lattice planes {*211*} of the α-Fe phase. The X-ray elastic constants $½s_2 = 5.76\ \text{TPa}^{-1}$, $s_1 = -1.25\ \text{TPa}^{-1}$ were used for the stress calculation. The experimental error given for each value is the standard deviation according to the "$\sin^2\psi$" residual stress calculation algorithm [3]. The residual stresses were obtained in the axial A and tangential T directions. Nevertheless, the axle axial direction is more important from the technological point of view and, in this direction, the main stresses occur. The FWHM value (Full Width at Half Maximum) was determined from the analysed diffraction line {*211*} at a tilt of $\psi = 0°$, error of determination does not exceed 0.05° 2θ.

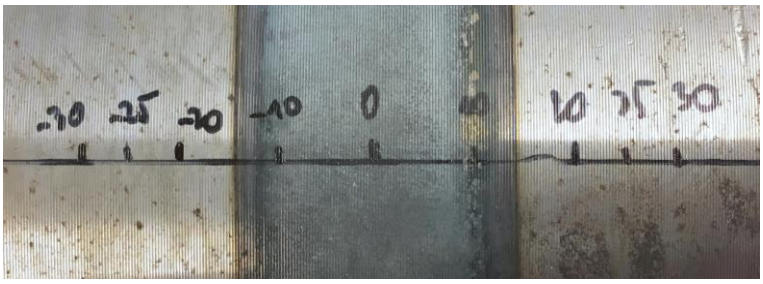

Fig. 2: Photo of hardened track, the numbers represent the distance from the track centre in millimetres

For the determination of the depth profiles of the macroscopic residual stresses, electrolytic etching of the surface layers of the material was used using a PROTO Electrolytic Polisher with the electrolyte A. The etched area was defined by a mask of Ø 14 mm. The depth of the removed layer was measured using a micrometre gauge.

Although results and analyses of residual stresses are the main subject of this paper, it is worthy to mention also fatigue resistance, which may be by residual stresses affected. Fatigue loading under press fits is very complicate and complex. Moreover, its simulation and experimental modelling are not easy and so it cannot be fully described and analysed within this paper, but some limited information about the experimental approach can be provided. As mentioned in the Introduction, two quite different fatigue mechanisms act on the surface of the axle seat under the press fit – "pure" high cycle fatigue and fretting fatigue. In this part of the investigations, only the first mechanism was studied. The problem was, how to simulate actual surface cyclic stresses, which are axial due to the bending loading of the axle in service. Eventually, after detailed analyses and considerations, it was decided that the best and likely also the only approach is to prepare three-point-bend specimens perpendicular to the surface laser track, with the laser track in the central part.

High-cycle fatigue tests were performed at different stress ranges to obtain the whole S-N curve including endurance limit. Load asymmetry was R = 0.1 (preloaded for security reasons), frequency 68 Hz. Test span was 80 mm. The central loading point was on the opposite side to the laser track. Cross section of the specimens was approximately 22 mm (height) x 20 mm (width).

Results and discussion

Cross-section of laser hardened track is shown in Fig. 3. The depth of track is 1.5–2 mm, which is sufficiently thick to affect the initiation and decelerate fatigue crack growth and friction corrosion cracks. Microstructure in laser-hardened track consists of martensite and retained austenite, see Fig. 4a. Under this full-transformed laser-hardened track, heat-affected zone (HAZ) formed by bainite and granular pearlite was observed, see Fig. 4b. The microstructure of the EA1N steel is ferritic-perlitic, see Fig. 4c - ferrite is equiaxial and fine with grain mean size 5.9 μm, colonies of pearlite has lamellar micromorphology.

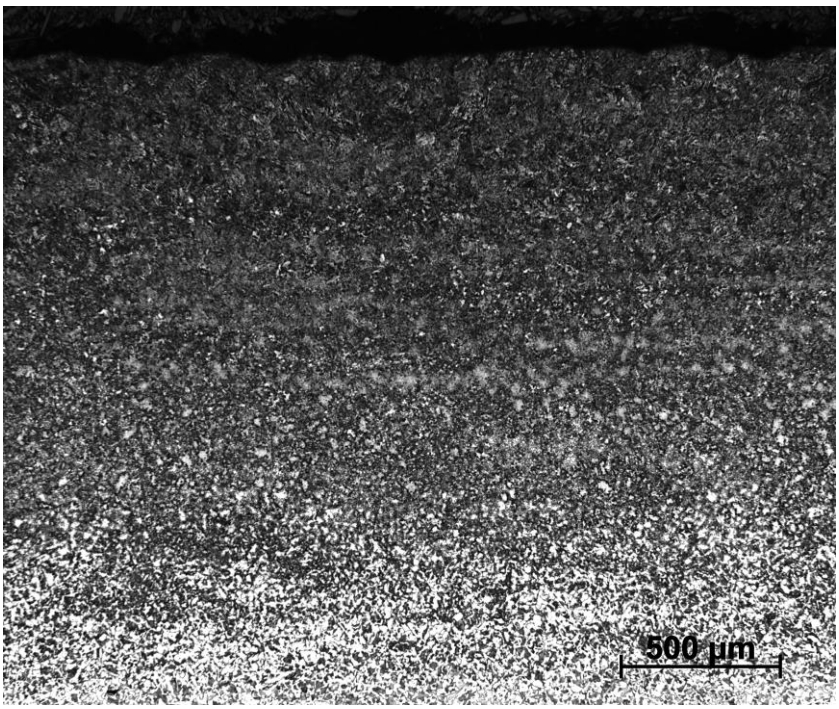

Fig. 3: Cross-section of laser hardened track

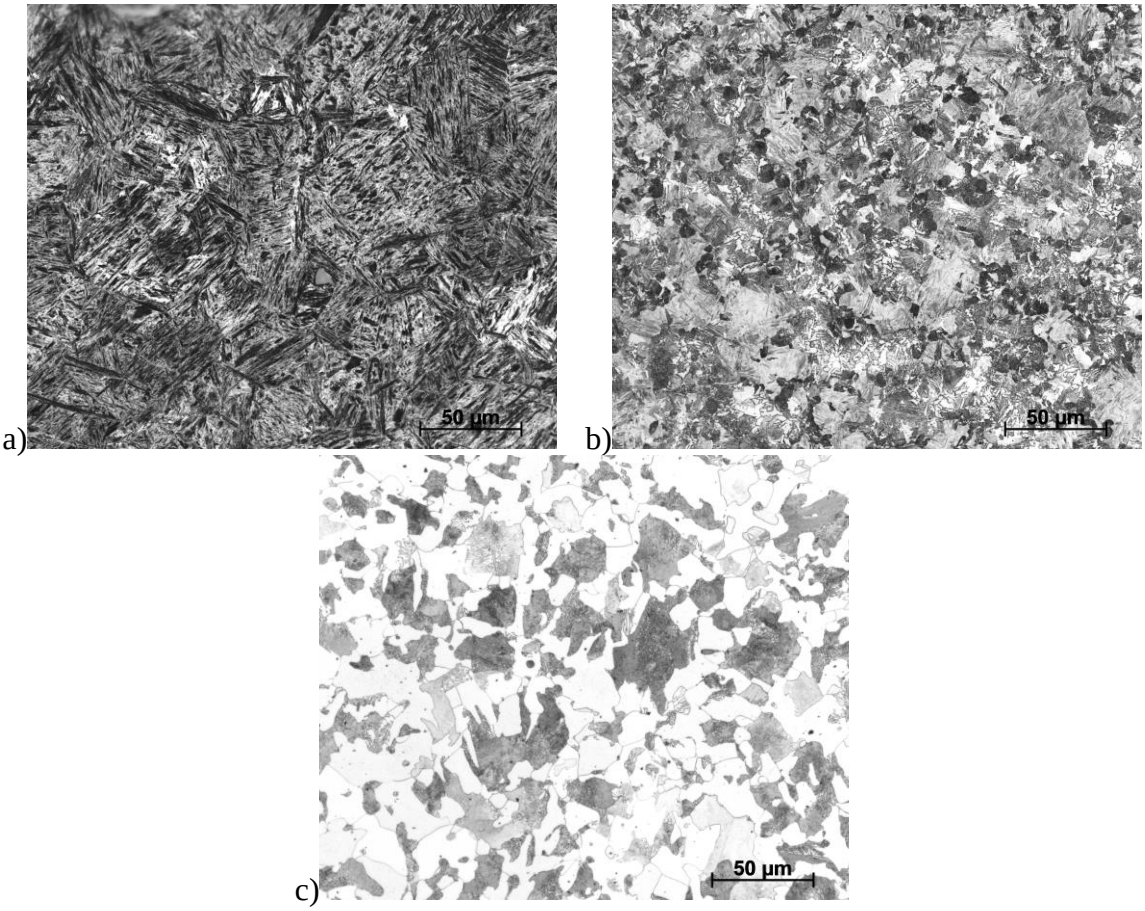

Fig. 4: Microstructure in: a) laser hardened track, b) HAZ and c) base metal

Analysed residual stresses on the surface of hardened track for the air-quenched (AQ) and also for the water-sprayed (WS) sample are compressive, on the contrary, residual stresses of bulk material (machined surface not affected by hardening, approx. 14 mm from the centre of hardened track) are tensile, see Fig. 5. The AQ sample shows slightly lower compressive residual stresses in the track, but this difference is not significant to compensate for the technological problems of quenching with a water spray. In addition, in the technologically significant direction A, the residual stresses are almost identical within the measurement inaccuracy as for the WS sample. Residual stresses of the bulk material vary by up to 400 MPa around the circumference, which is most likely caused by the production of the semi-finished product. However, the average value of 72 residual stress measurements around the circumference of the AQ sample in the middle of the hardened track is –101 ± 45 MPa. Therefore, the state of the residual stress after laser hardening is homogeneous around the circumference.

The FWHM values of the bulk material are homogeneous within the error, see Fig. 6. The FWHM values are higher in the hardened track compared to the bulk material. This could be a result of higher microdeformation and/or dislocation density, and/or smaller crystallite size. Additional experiments, especially diffraction phase analysis, are needed to identify the cause. Sharp maxima of the FWHM values approx. 10 mm from the hardened track axis can be caused by a step change of the diffraction angle of the {*211*} planes. Due to the size of the irradiated area and the radiation beam divergence, the irradiated areas diffract with both the "smaller" and "larger" diffraction angles, resulting in an increase in the FWHM parameter. The step change in diffraction angle is caused by a change in the material microstructure between the bulk material (ferrite-pearlite) and the hardened area (martensite and retained austenite). The FWHM

values of the bulk material of the samples are identical. Thus, the microstructure of the bulk material is homogeneous, however, the residual stresses vary.

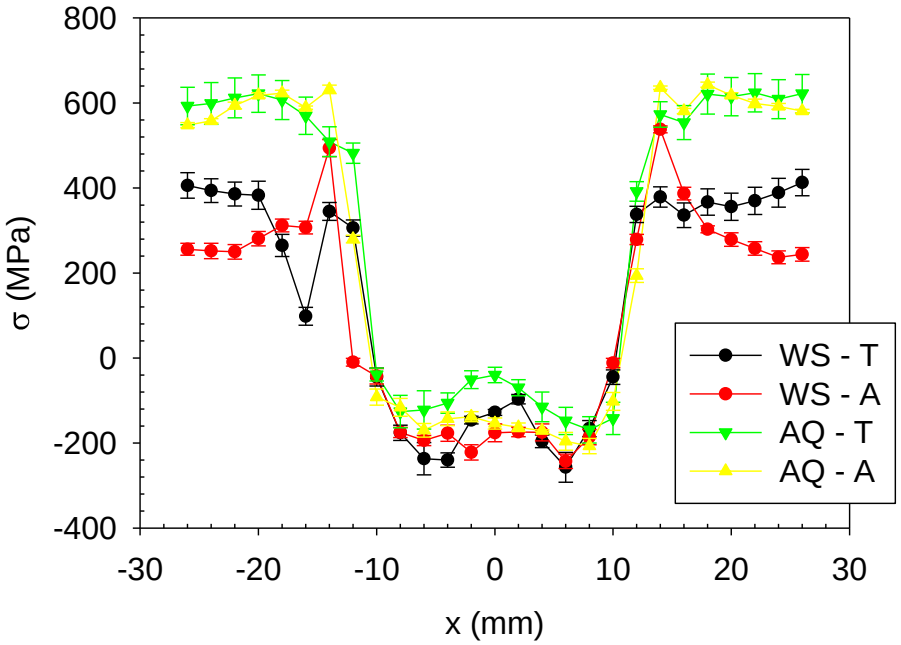

Fig. 5: Distribution of surface macroscopic residual stresses across the hardened track for air-quenched (AQ) and water-sprayed (WS) sample in the axial (A) and transversal (T) direction

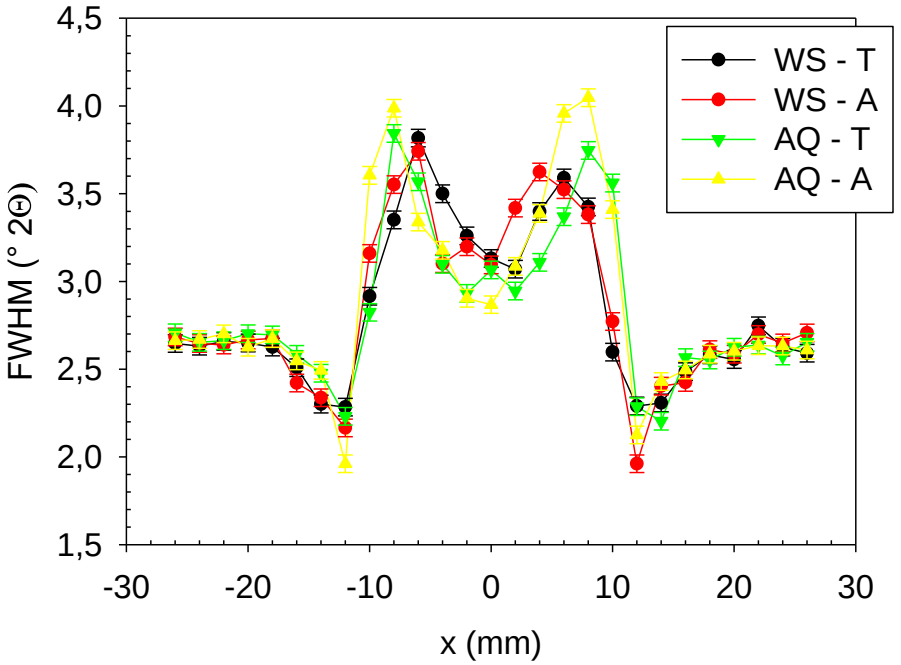

Fig. 6: Distribution of FWHM values across the hardened track for air-quenched (AQ) and water-sprayed (WS) sample in the axial (A) and transversal (T) direction

The depth profiles of the macroscopic residual stresses and FWHM values in axial direction are almost identical for both investigated samples, see Fig. 7. Compressive residual stresses up to a depth of ca 200–300 µm are an important positive factor for the fatigue resistance of the axles under operation. Compressive residual stresses of the WS sample are approx. 50 MPa higher than in the case of the AQ one. The greatest difference can be seen in the 300 µm thick

surface layer. FWHM values are approx. 0.1° 2θ higher compared to AQ sample. These differences are not significant in terms of measurement accuracy, and again, slither higher compressive residual stress values do not justify the use of technologically more complicated quenching with a water spray. From the depth approx. 1000 µm the values of residual stresses and 1500 µm for FWHM are stable. The decrease in FWHM values indicates a decreasing microdeformation, dislocation density and/or increasing crystallite size. Low FWHM values refer to coarser grained bulk material, see Fig. 4.

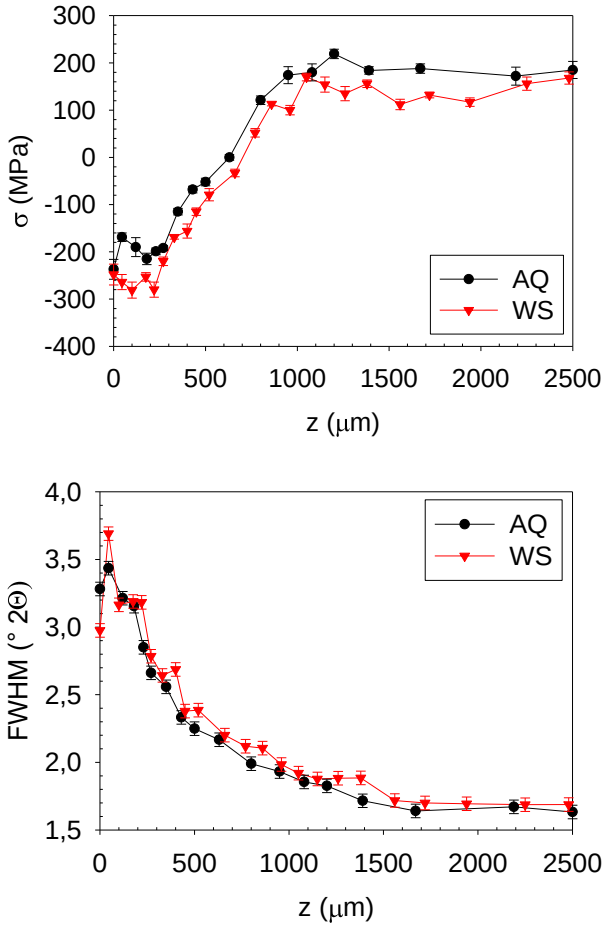

Fig. 7: Depth profiles of the macroscopic residual stresses and FWHM values for air-quenched (AQ) and water-sprayed (WS) sample in axial (A) direction

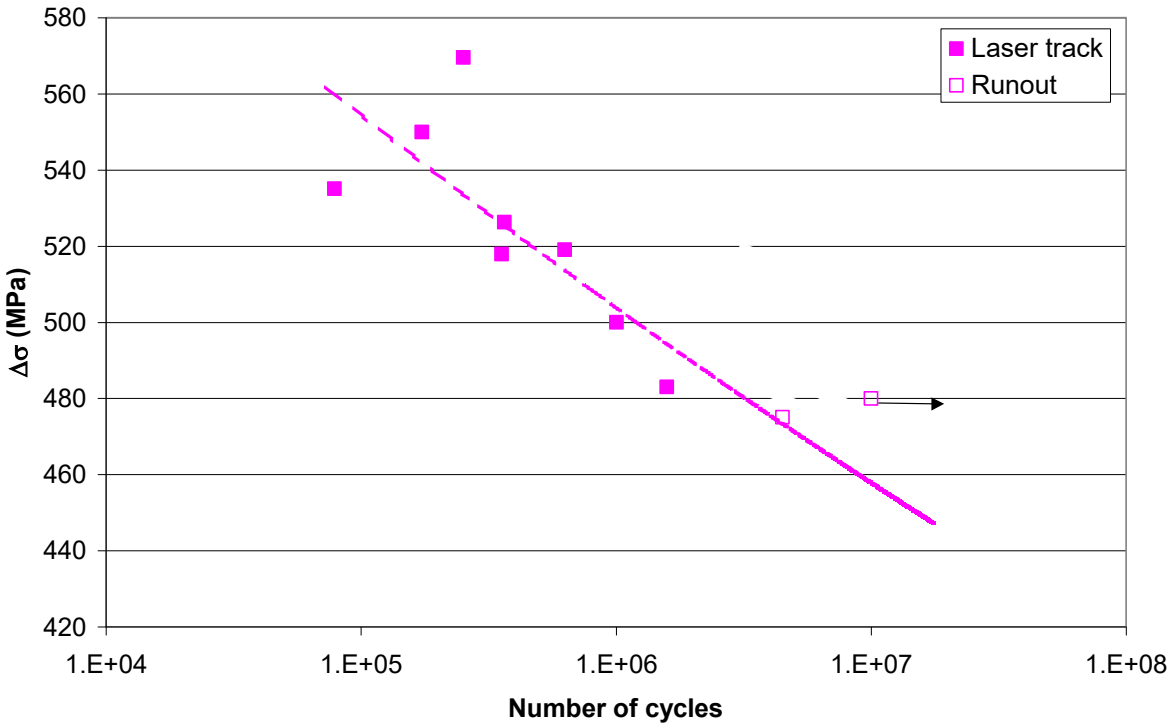

Fig. 8: Results of the high-cycle fatigue tests

Results of the first stage of high-cycle fatigue tests are in Fig. 8. During these tests, with the central load point exactly opposite the centre of the laser track, failure occurred always at the track centre. So, the diagram represents fatigue strength of the laser treated surface itself, not the boundary between the track and untreated material.

Though it is not easy to recalculate fatigue strength for different load asymmetries, the results are encouraging. The first estimations indicate that fatigue strength of the full axle will be higher than requested by railway standards and higher than for laser untreated axle. This is consistent with the measurement of residual stresses, where in the centre of the track, compressive stresses favourable for fatigue resistance occurred, see Fig. 5. Note, however, that the critical area of premature failure likely will be the boundary between the track and untreated material.

Conclusions

In terms of fatigue failure of the axle seats, compressive residual stresses in the surface layers of the laser track in the axial direction can be evaluated as the most valuable. With the optimized position of the laser tracks on the inner edge of the axle seats, these compressive stresses can play a crucial role in the process of retardation or even complete arrest of physically short cracks, thereby significantly increasing the fatigue resistance of the axles under operation. The paper is completed by results of high-cycle fatigue tests indicating a significant increase of fatigue strength inside laser traces on one hand and partial reduction of fatigue strength in the area of boundaries between the laser trace and untreated surface.

Acknowledgements

Measurements were supported by the project TH04010475 of the Technology Agency of the Czech Republic. This work was supported by the Grant Agency of the Czech Technical University in Prague, grant No. SGS19/190/OHK4/3T/14.

References

[1] G. Gürer, C. H. Gür, Failure Analysis of Fretting Fatigue Initiation and Growth on Railway Axle Press-Fits, Eng. Fail. Anal. 84 (2018) 151–166.

[2] V. Linhart, I. Černý, An Effect of Strength of Railway Axle Steels on Fatigue Resistance Under Press Fit, Eng. Fract. Mech. 78 (2011) 731–741.

[3] I. Kraus, N. Ganev, Residual Stress and Stress Gradients, in: Industrial Applications of X-Ray Diffraction, New York, USA, 2000, pp. 793–811.